Native oxide on ultra-thin NbN films

A.V. Lubenchenko[1*], A.B. Pavolotsky[2&], S. Krause[2], O.I. Lubenchenko[1], D.A. Ivanov[1], V. Desmaris[2], V. Belitsky[2]

Abstract—**We report study of native oxide formation over NbN ultra-thin films. With a help of XPS, chemical and phase depth profiles of NbN film of 5 nm and 10 nm thickness exposed to room air for more than a month were recorded. The surface of those films were sputtered with Ar^+ ions and consequently oxidized in room air for another few days. It was found that an intermediate layer of NbN_x was formed between the niobium oxide layer and original NbN material.**

I. Introduction

Ultra-thin NbN film is a material, on which the modern state-of-the-art sensitive devices like hot-electron bolometers (HEB) [1], [2] and superconducting single-photon detectors (SSPD) [3], [4] are based. The performance of such devices largely depends on the material properties of the NbN film, its chemical and phase composition as well as their depth profiles.

As-deposited films are always strained due to a mismatch of crystal lattices of the substrate and the film, as well as due to the difference of thermal expansion coefficients. The stress relaxation and reconstruction of thin films lead to structural transformation of the film itself, as well as the formation of various phases of variable composition and interfaces between them. During the process of device fabrication, the NbN film always gets exposed to room air, which causes formation of the native oxide layer over it. The native oxide layer is often left present in the final device structure between the NbN superconducting layer and the contact metallization layers. On the other hand, native oxide layer effectively withdraws part of the ultra-thin layer thickness from being a superconducting NbN material. The knowledge of the chemical and phase profiles of NbN film deposited on a certain substrate are crucial for proper understanding of the devices and their designing.

II. Experimental Details

NbN films of 5 nm and 10 nm thickness were deposited onto a silicon substrate by reactive magnetron sputtering in the AJA Orion-5-U-D sputtering system [5], [6]. The film thickness during sputtering was controlled by the known sputtering rate (the sputtering rate was verified by HRTEM of the films).

The X-ray photoemission spectroscopy (XPS) studies of the samples surfaces were performed with the help of the electron-ion spectroscopy module based on the Nanofab 25 (NT-MDT) analytic platform. In the analysis chamber, oil-free ultrahigh vacuum was kept at the level of about 10^{-7} Pa. The X-ray source SPECS XR 50 without a monochromator with Mg anode as the X-ray source (1253.6 eV photon energy) was used. The spectra were recorded with a help of electrostatic hemispherical energy analyzer SPECS Phoibos 225. The energy resolution based on the full width at half maximum (FWHM) of the spectrometer at the Ag3d5/2 line (peak) was 0.78 eV for non-monochromatic X-radiation Mg Kα. The energy positions of the spectra peaks were calibrated with reference to the Cu2p3/2 (binding energy 932.62 eV), Ag3d5/2 (368.21 eV) and Au4f7/2 (83.95 eV) peaks. All survey spectra scans were recorded at a pass energy of 80 eV. The detailed scans of strong lines were in most cases recorded as wide as needed just to encompass the peak(s) of interest and were obtained with a pass energy of 20 eV. The energy analyzer was operated in Fixed Analyzer Transmission (FAT) mode.

The ion source SPECSIQE 12/38 was used for sputtering the samples. The ion source had differential pumping and was fed with 99.9995% pure Ar. The ion beam scanned an area of 2.8 mm × 4.0 mm at the incidence angle of 70° to the surface normal, the ion beam energy was of 500 eV.

III. Chemical and Phase Profile Analysis

X-ray photo-electron spectroscopy (XPS) is one of the most efficient non-destructive methods of ultrathin films surface chemical and phase analysis. In the standard XPS realization, relative concentrations of the chemical elements are calculated with the assumption of uniform concentration of the elements across the whole depth of analysis.

Real surfaces though are always non-uniform and multi-component across the depth. Ignoring these facts cause significant inaccuracy of the analysis and often makes the extracted information questionable.

In most cases, the sample's surface not only is multilayered, but also consists of the layers of different chemical and phase composition. The extraction of the surface layer chemical and phase information from XPS spectra is a complex reverse problem with multiple unknown parameters.

In the present work, we followed the approach from [7] for XPS analysis of the oxidized surface of NbN ultrathin film. It suggests (1) the novel method for extraction of the background due to multiple inelastic electron scattering, (2) new XPS line decomposition into the component peaks accounting for

[1] National Research University MPEI, Krasnokazarmennaya, 14, Moscow 111250, Russia

[*] Corresponding author, email: LubenchenkoAV@mpei.ru

[2] Chalmers University of Technology, Group for Advanced Receiver Development, Department of Space, Earth and Environment, Göteborg, 412 96, Sweden

[&] Corresponding author, email: Alexey.Pavolotsky@chalmers.se

physical meaning of the decomposition parameters and jointly with background extraction, and (3) extracts the layer thicknesses following the simple formula.

The method assumes that the sample surface consists of a number of flat and parallel layers, each of them is uniform and can be multicomponent. Such assumption is justified by the fact that the lateral dimensions of the analyzed area are by many orders of magnitude larger than the analysis depth. Because of that, lateral non-uniformities of the surface under analysis (e.g. islands, nanoscale precipitations, elements of interface topography) are naturally averaged across the lateral dimensions. This way, structural non-uniformity will be characterized by relative concentration of chemical elements of a particular phase contained in a layer of a certain thickness.

The studied ultrathin films were deposited in vacuum. Consequent unloading the samples to the room air caused oxidation of the sample surface. As the oxidation progresses from the sample's outer surface towards its depth, the highest oxidation state will be at the immediate top surface of the film and will decrease along the sample's depth. Also, storage of the samples in the room conditions unavoidably causes hydrocarbons to deposit over the film surface.

Layer thicknesses will be calculated by the formula [7]:

$$d_i = \lambda_i \cos\theta \ln\left(\frac{I_i/(n_i\omega_i(\gamma)\lambda_i)}{\sum_{j=0}^{i-1} I_j/(n_j\omega_j(\gamma)\lambda_j)} + 1\right) \qquad (1)$$

where d_i is the thickness of the i-th layer, n is the atomic concentration, $\omega_i(\gamma)$ is the differential cross-section of photoelectron production [8], γ is the angle between the directions of incident radiation and to the energy analyzer, λ is the IMFP (IMFP is calculated by the TPP2M formula [9]), θ is the angle between the direction to the energy analyzer and the surface normal, I_i is the i-th peak intensity. The layers will be numbered upwards toward the surface.

IV. Results and Discussion

In this work, we studied the influence of air oxidation onto the composition profile of NbN ultra-thin films. After deposition, the film samples were covered with an oxidation-protective layer. This layer was fully removed before the analysis in ultrasonic bath with acetone, and after that with isopropanol. The procedures of cleaning and loading samples into the analysis chamber took about 10 minutes. So the samples were air-exposed for less than 20 minutes total. The results of analysis of such films were earlier communicated in [6]. The oxidized layer thickness did not exceed 2 nm. The niobium oxide's composition was found to be NbO_2. In this work, we studied films that had been oxidized for more than a month after removing the protective layer. During that time the film structure changed dramatically: not only the oxide layer became thicker, up to ca. 3 nm thick, but the niobium oxide became Nb_2O_5.

Ion sputtering was used for removing of the surface oxide layer. Ion sputtering was done in the number of 20 minutes long steps each followed by XPS analysis. Each sputtering step removed a few monolayers. After 5th sputtering step, the highest oxide, i.e. Nb_2O_5, was completely removed. The mean ion

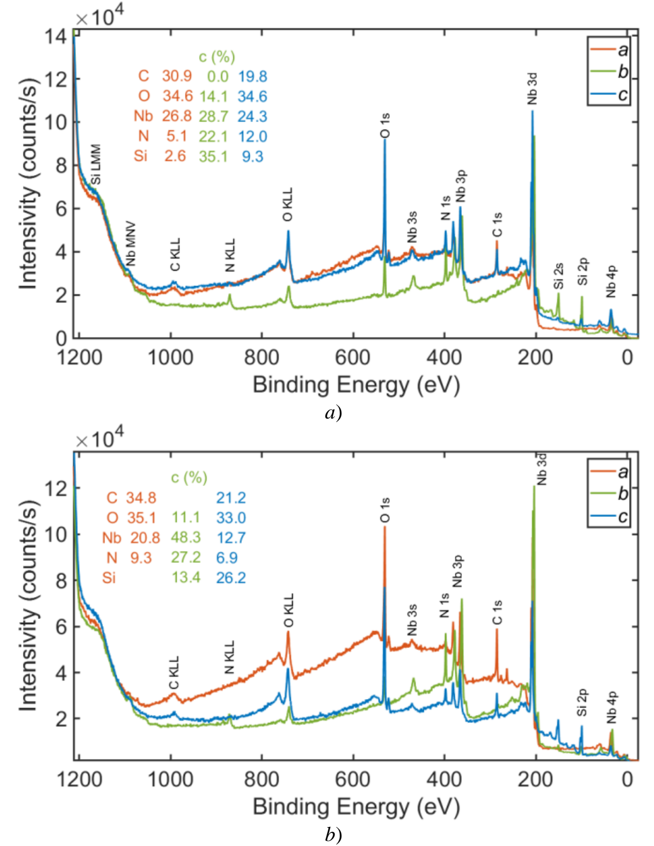

Fig. 1. Survey XPS spectra. Target: *a)* NbN, 5 nm; *b)* NbN, 10 nm. Line: (a) NbN films of 5 nm and 10 nm thickness after >1 month exposed to room air; (b) the same films after Ar^+ sputtering; (c) after consequent air oxidation for another few days.

penetration depth was about 1 nm, and consequently, the thickness of the modified layer was less than 2 nm. After oxide sputtering, the samples were unloaded from the analysis chamber and exposed to oxidation in air for a few days.

The following samples were analyzed by XPS: (a) NbN films of 5 nm and 10 nm thickness after more than 1 month exposure to room air; (b) the same films after Ar^+ sputtering; (c) after consequent air oxidation for another few days. A standard XPS analysis showed presence of C, O, Nb and Si in the samples. Fig. 1 shows the survey spectra and presents the relative atomic concentrations of the elements in the samples with 5 and 10 nm thick NbN films after each sputtering step.

To analyze composition and chemical bond, the XPS line of an element of interest needs to be decomposed into component peaks. The XPS line structure can be quite complex due to superposition of peaks of the element in its different chemical bond states and presence of satellite peaks. Moreover, shape

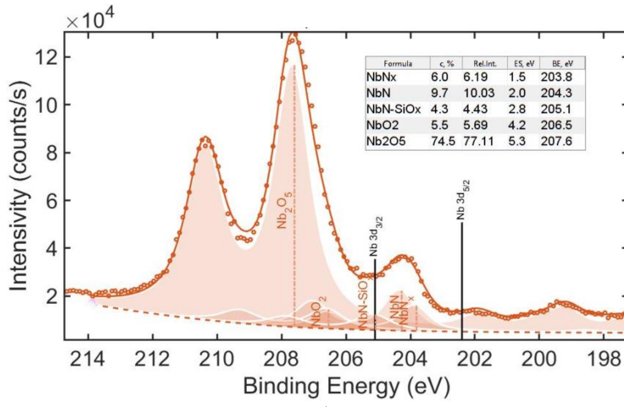

a)

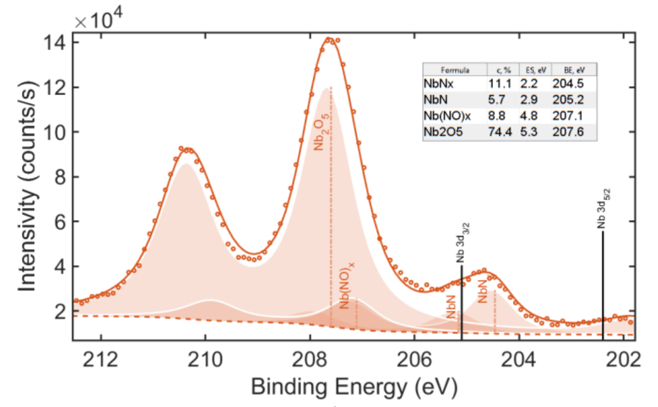

a)

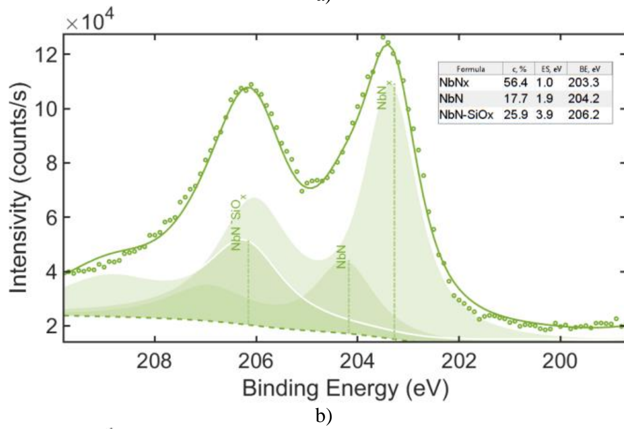

b)

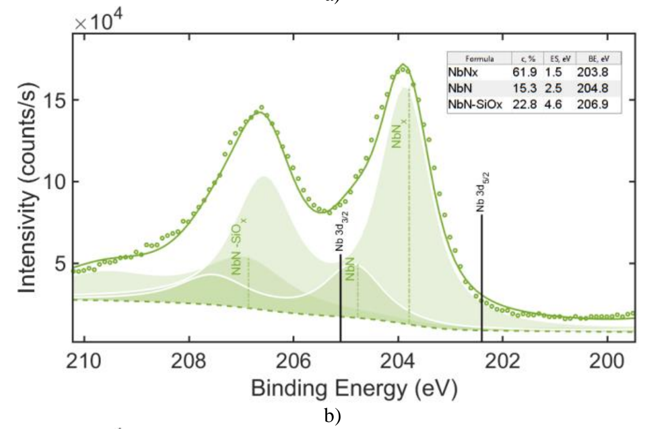

b)

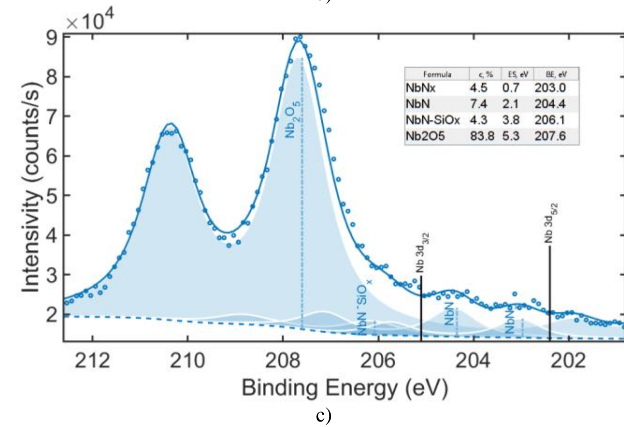

c)

Fig. 2. XPS spectra of line Nb 3d. Target: a) NbN films of 5 nm thickness after >1 month exposed to room air; b) the same films after Ar^+ sputtering; c) after consequent air oxidation for another few days. Solid lines: calculation. Circles: experimental data. Area: separate calculated peaks.

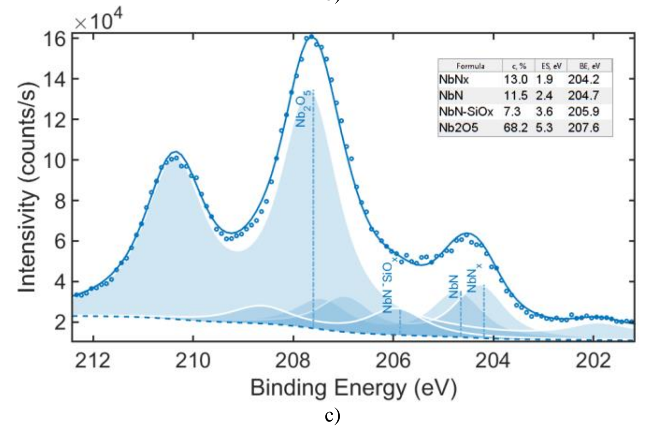

c)

Fig. 3. XPS spectra of line Nb 3d. Target: a) NbN films of 10 nm thickness after >1 month exposed to room air; b) the same films after Ar^+ sputtering; c) after consequent air oxidation for another few days. Solid lines: calculation. Circles: experimental data. Area: separate calculated peaks.

and width of the peaks could be affected by a various factors. For XPS peaks deconvolution, we followed the approach presented in [7].

The spectral line shape is defined by convolution of functions describing natural shape of the line and instrumental broadening. We describe the natural shape of the line with a Doniach-Sunjic relation, while the instrumental broadening follows Gauss' function. We suggest usage of the binding energy and spin-orbit interaction energy numbers from a reference book [10]. The chemical shift energy is almost linearly proportional to the oxidation state, hence, it is sufficient to find the chemical shift energy of element with highest oxidation state, e.g. we used chemical shift energy 5.31 eV for Nb_2O_5. The chemical shift energy of Nb-N compounds strongly depends on their stoichiometry. The chemical shift energy dependence on the stoichiometric coefficient x for the lines Nb 3d and N 1s in NbN_x compounds is shown in the paper [11].

Fig. 2 and Fig. 3 present the results of Nb 3d spectral line decomposition into different phase component peaks for the samples of 5 and 10 nm thick NbN films after each analysis stage, respectively.

For the samples of NbN films, 5 nm and 10 nm thick, after more than 1 month exposure to room air, there were two niobium nitride phases identified: NbN and NbN_x, $x \approx 0.79$ corresponding probably to Nb_5N_4. The stoichiometric coefficient x was extracted from the chemical shift energy with

TABLE I
CHEMICAL AND PHASE DEPTH PROFILE OF AN ULTRA-THIN NIOBIUM NITRIDE FILM 5 NM

	Formula	d (nm)		
		a	b	c
5	hydrocarbons	1.0	-	0.8
4	Nb_2O_5	3.2	-	2.5
3	NbN_x	1.5	1.8	0.1
2	NbN	3.5	0.5	0.1
1	Nb-SiO_x	1.2	1.6	2.2
	Si	substrate		

TABLE II
CHEMICAL AND PHASE DEPTH PROFILE OF AN ULTRA-THIN NIOBIUM NITRIDE FILM 10 NM

	Formula	d (nm)		
		a	b	c
5	hydrocarbons	0.6	-	0.8
4	Nb_2O_5	5.2	-	2.4
3	NbN_x	2.2	2.0	0.6
2	NbN	not re-	1.1	0.6
1	Nb-SiO_x	corded	1.4	1.6
	Si	substrate		

a use of the data from [11]. The peak position in the line Nb 3d shifts towards the lower binding energy numbers after sputtering (Fig. 2). This points to the fact that stoichiometric coefficient *x* in niobium nitride compound NbN_x in the film shifts towards lower number. Apart of the two nitride phases, the analysis identified the presence of complex oxi-nitride compound Nb-SiN_xO_y. This oxi-nitride could only be formed at the early stage of NbN film growth on the covered by silicon native oxide substrate.

Finally, based on the results of the XPS line decomposition and following the Eq. (1), chemical composition and phase depth profiles were extracted for each stage of the surface analysis (Tables I and II): (a) NbN film of 5 nm end 10 nm thickness after more than 1 month exposure to room air, (b) the same films after Ar^+ sputtering, and (c) after consequent air oxidation for another few days.

V. CONCLUSION

In this work, we studied films that had been oxidized for more than a month after removing the protective layer. During that time the film structure changed dramatically: not only the oxide layer became thicker, ca. 3 nm thick, but the niobium oxide became Nb_2O_5. Moreover, a non-stoichiometric niobium nitride NbNx, ca. 1 nm thick, was found between Nb_2O_5 and the stoichiometric NbN layers. Further, the oxide was removed by a “delicate” Ar+ ion sputtering. After sputtering, the samples were again exposed to a room air for a few days. That caused formation of the oxide layer of Nb_2O_5 about 2 nm thick, and about a monolayer of non-stoichiometric NbN_x phase under it.

REFERENCES

[1] D. Meledin *et al.*, “A 1.3-THz balanced waveguide HEB mixer for the APEX telescope,” *IEEE Trans. Microw. Theory Tech.*, vol. 57, no. 1, 2009.

[2] S. Krause *et al.*, “Noise and IF Gain Bandwidth of a Balanced Waveguide NbN / GaN Hot Electron Bolometer Mixer Operating at 1 . 3 THz,” *IEEE Trans. Terahertz Sci. Technol.*, vol. 8, no. 3, pp. 365–371, 2018.

[3] G. N. Gol’tsman *et al.*, “Picosecond superconducting single-photon optical detector,” *Appl. Phys. Lett.*, vol. 79, no. 6, pp. 705–707, Aug. 2001.

[4] A. Verevkin *et al.*, “Ultrafast superconducting single-photon detectors for near-infrared-wavelength quantum communications,” *J. Mod. Opt.*, vol. 51, no. 9–10, pp. 1447–1458, Jun. 2004.

[5] S. Krause *et al.*, “Epitaxial growth of ultra-thin NbN films on Al $_x$ Ga $_{1-x}$ N buffer-layers,” *Supercond. Sci. Technol.*, vol. 27, no. 6, 2014.

[6] S. Krause *et al.*, “Ambient Temperature Growth of Mono-and Polycrystalline NbN Nanofilms and Their Surface and Composition Analysis,” *IEEE Trans. Appl. Supercond.*, vol. 26, no. 3, 2016.

[7] A. V. Lubenchenko, A. A. Batrakov, A. B. Pavolotsky, O. I. Lubenchenko, and D. A. Ivanov, “XPS study of multilayer multicomponent films,” *Appl. Surf. Sci.*, vol. 427, 2018.

[8] J. J. Yeh and I. Lindau, “Atomic subshell photoionization cross sections and asymmetry parameters: $1 \leqslant Z \leqslant 103$,” *At. Data Nucl. Data Tables*, vol. 32, no. 1, pp. 1–155, Jan. 1985.

[9] S. Tanuma, C. J. Powell, and D. R. Penn, “Calculation of electron inelastic mean free paths (IMFPs) VII. Reliability of the TPP-2M IMFP predictive equation,” *Surf. Interface Anal.*, vol. 35, no. 3, pp. 268–275, Mar. 2003.

[10] J. F. Moulder, W. F. Stickle, P. E. Sobol, and K. D. Bomben, *Handbook of X-Ray Photoelectron Spectroscopy. A Reference Book of Standard Spectra for Identification and Interpretation of XPS Data*. Eden Prairie, MN: Physical Electronics, 1995.

[11] P. Prieto, L. Galán, and J. M. Sanz, “An XPS study of NbNx prepared by ion implantation and the near-surface effects induced by Ar+ bombardment,” *Surf. Sci.*, vol. 251–252, pp. 701–705, Jul. 1991.